A Voltage-Measurement Based Estimator for Current and Temperature in MOSFET H-Bridge

Cyril Buttay, Dominique Bergogne, Hervé Morel, Bruno Allard, René Ehlinger, Pascal Bevilacqua

A Voltage-Measurement Based Estimator for Current and Temperature in MOSFET H-Bridge

Buttay Cyril, Bergogne Dominique, Morel Hervé, Allard Bruno,
Ehlinger René and Bevilacqua Pascal
CEGELY-INSA, Bât. Léonard de vinci
Av. Capelle ouest
69621 Lyon, France
+33 (0)4 72 43 82 38
buttay@cegely.insa-lyon.fr

Abstract – This paper describes a method to extract internal temperature and drain current values of a MOS transistor by proceeding to voltages acquisitions only. Two current and temperature dependant voltages are measured: the drain-to-source voltage when the MOSFET is in the linear state, and the body diode forward voltage drop when freewheeling.

Analytical expression are proposed to estimate temperature and current values from the voltages measurements. The method is then implemented in a microcontroller to achieve a low cost monitoring system.

Accuracy of the system is verified, and confidence maps over the full working range of the devices are given.

An application to chip-to-ambient thermal impedance measurement using the estimator and a calorimeter is proposed.

Keywords: Device characterisation, Diagnostics, Estimation techniques, Measurements, MOS device, Sensors

1. Introduction

The increasing usage of power converters in today's world make their market more challenging. Cost cuts are of major concern to remain competitive, but reliability requires expensive security margins. Monitoring is another solution to keep converters reliable while using power components closer to their limits. However, the monitoring of critical values (i.e. Current and Temperature) is either costly or inaccurate. Shunts are widely used in low power converters to measure current, but as power increases, losses in the shunt become not negligible, reducing efficiency. Transformer-based current probes are expensive, bulky and their frequency bandwidth is often an issue. In the other hand, temperature measurements can be made affordable, by using a thermistor close to the transistors. This is however inaccurate because substrate temperature and device temperature are sometimes different, especially during large power surge.

Estimation is an other way to figure out temperature and current values by measuring some variables of the device under monitoring. Extensive work and literature relate techniques based upon an estimator to avoid the cost and pitfalls of dedicated sensors [1-3]. The method proposed in this paper is based on the measurement of the drain-to-source voltage at the terminals of one MOSFET in an inverter.

Two temperature and current-dependent voltages are used for the estimation. When in the on-state, drain-to-source voltage of a MOSFET is equal to the intrinsic on-state resistance (R_{DSon}) multiplied by the drain current. As R_{DSon} is temperature-dependent, drain-to-source voltage is a function of current and temperature. When frewheeling on its internal body diode, the MOSFET drain-to-source voltage is equal to the diode forward voltage, also dependent on temperature and current.

Thanks to the proximity of the body diode and the channel (a few µm), the temperature can be supposed to be identical in both areas. Assuming both measurements are performed within a short lapse of time (in comparison to thermal constants in the device), and providing a relation between the two currents in the two states, it is possible to extract the temperature and current values. In this paper, we consider that temperature is constant across the silicon die. It is referred to as “chip temperature".

2. Principle of operation

In a classical inverter, a dead-time is observed between the turn-off of a pair of switches (e.g. H1 and L2, as described on fig. 1) and the turn-on of the opposite pair (i.e. H2 and L1). Given the load is inductive, current flows through body diodes of H2 and L1, which will therefore act as freewheeling devices during this period. To achieve high efficiency, the dead-time must be as short as possible to reduce the voltage drop across the body diode. Transients caused by commutation last longer than the dead-time, masking the freewheeling diodes forward voltage drop, which cannot therefore be measured at this time. Forward-voltage measurement is performed by turning-off the transistor L1 a short lapse of time after the beginning of its conduction. This will not disturb the operation of the inverter, as it doesn't involve a high voltage step (less than 1V) nor high current gradient (the only change in the current path is across the silicon die). This turning-off must be done before the current I_D becomes positive in the switch (with respect to the conventions below), otherwise it would flow through the diodes of H1 and L2.

The measurement of the drain-to-source voltage (in the resistive on-state) will be performed just before the end of the conduction, to ensure a good signal-to-noise ratio (the current is maximal at the end of the conduction cycle).

3. Analytical approach

Drain-to-source voltage is measured in two working states to achieve temperature and current estimation. In this section, we present the analytical expressions linking the voltage and the parameters being estimated in each state

A. On-state resistance model

The effect of temperature on the on-state MOSFET resistance, is quite well taken into account by classical models such as those implemented in SPICE.

For the sake of simplicity, the equations given here are those of the SPICE level1 MOS model[4].

In the linear region, i.e. $V_{GS} > V_{TH}$ and $V_{DS} < V_{GS}-V_{TH}$,

$$I_D = KP\,\frac{W}{L-2X_{jl}}\left(V_{GS}-V_{TH}-\frac{V_{DS}}{2}\right)V_{DS}\left(1+\lambda V_{DS}\right) \tag{1}$$

Where KP is the transconductance parameter, W and L respectively the width and length of the

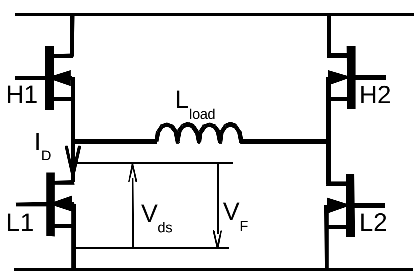

fig. 1 Conventions

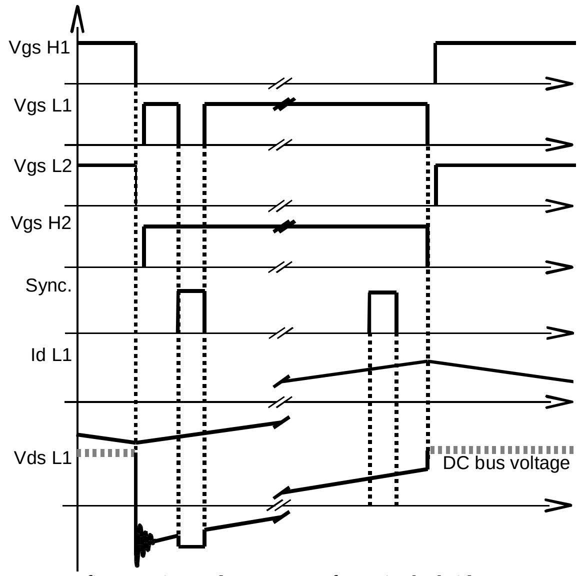

fig. 2. Drive and power waveforms in the bridge

channel, X_{jl} the metallurgical junction depth, V_{GS} the gate to source voltage, V_{TH} the gate to source threshold voltage, and λ is the channel length modulation.

For power MOSFETs, λ is considered as zero. KP can be supposed to be the only temperature dependent parameter,

$$KP(T_2) = KP(T_1)\left(\frac{T_1}{T_2}\right)^{\frac{3}{2}} \tag{2}$$

The influence of the temperature on the on-state resistance is given by replacing (2) into (1), and then deriving.

$$\frac{\partial I_D}{\partial V_{DS}} = KP(T_1)\left(\frac{T_1}{T_2}\right)^{\frac{3}{2}} \frac{W}{L-2X_{jl}}\left(V_{GS} - V_{TH} - V_{DS}\right) \tag{3}$$

Notice that R_{DSon} evolves as a 1.5 power of the temperature. On a reduced temperature range, this can therefore be approached as a 2nd order polynomial.

$$R_{DSon} = C_0 + C_1 T + C_2 T^2 \tag{4}$$

B. Intrinsic body diode forward-voltage model

As it can be seen in the extensive literature, there are few simple but accurate formulations of the diode forward-voltage drop [5-7]. This is due to the great number of phenomena occurring in a classical PIN diode. Ohmic contacts are of a major concern in this voltage drop, although they are hardly taken into account in numerous models. The temperature and doping gradients across the PN junction have also an influence, but are difficult to quantify.

In [5], an analytical expression is used to determine the junction temperature of a power diode from its forward-voltage and current, but is far too complex for the targeted application.

Thought for monitoring the proposed method does not require high accuracy. The chosen model is therefore as simple as the following first-order polynomial of I:

$$V_F = V_S(T) + K_2 I \tag{5}$$

where $V_s(T)$ is the temperature dependant threshold voltage, and K_1 a fixed coefficient.

$$V_S = K_0 + K_1 T \tag{6}$$

Therefore

$$V_F = K_0 + K_1 T + K_2 I \tag{7}$$

C. Temperature and current expressions

From (4) it comes, when in the on-state:

$$V_{DS1} = R_{DSon} I$$

$$V_{DS1} = \left(C_0 + C_1 T + C_2 T^2\right) I_1 \tag{8}$$

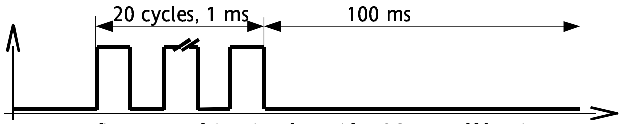

fig. 3 Burst drive signals avoid MOSFET self-heating

when in the “freewheeling” mode, (7) yields to

$$V_{DS2} = -V_F = -K_0 - K_1 T - K_2 I_2 \tag{9}$$

V_{DS1} is measured at the beginning of the conduction period, while V_{DS2} is the value of the drain-to-source voltage at the end of the conduction. I_1 and I_2 are therefore different, but T can be considered as constant, due to the high thermal time constant (the self-heating will directly be taken into account in the parameter fitting).

When using a pure inductive load, I_1 and I_2 are linked by:

$$I_2 = I_1 - \frac{U\,\Delta t}{L_{load}} \tag{10}$$

where Δt is the time interval between the set of two data acquisitions, U is the DC-bus voltage, and L_{load} the load inductance. From (9), it comes:

$$I_2 = -\frac{V_{DS2} + K_0 + K_1 T}{K_2} \tag{11}$$

Using (10) and (11) in (8) yields:

$$V_{DS1} = \left(C_0 + C_1 T + C_2 T^2\right)\left(\frac{U\,\Delta t}{L_{load}} - \frac{V_{DS2} + K_0 + K_1 T}{K_2}\right) \tag{12}$$

T is therefore obtained by solving the third order polynomial (12). (11) gives the corresponding I_2 value.

4. Parameter estimation

A. Description of the experimental setup

An inverter is built for demonstration purposes. It operates at constant frequency and duty cycle, and the load is a low-value inductance. Theses experimental conditions ensure a pure-AC triangular-shaped load current, allowing for both voltage measurement (V_F and V_{DSon}) to occur within a short lapse of time. The transistors of the bridge are 75V, 100 A rated devices.

The inverter (H-bridge) is driven using burst signals, to keep transistors self-heating as low as possible, and Insulated Metal Substrate (IMS) is used to guarantee the best thermal spreading. This bridge is placed into a furnace to set the ambient temperature. With this setup, we can assume chip temperature to be equal to ambient temperature at the equilibrium. However, passive components of the inverter (input capacitor bank and inductive load) cannot withstand temperatures up to 180°C and have to be kept out of the furnace. This results in a non-negligible stray inductance along the circuit. This has a detrimental effect on the linearity of the current waveform (see fig. 4)

The drain-to-source voltage is acquired using two P6139 500MHz passive probes in a differential setup and a TDS7054 Tektronix digital oscilloscope. Current is measured with a Pearson Electronics model 101, 80MHz bandwidth current transformer. Drain-to-ground and source-to-ground voltages were clamped using zener diodes to avoid saturation of the oscilloscope input amplifiers.

Temperature is acquired as the average value given by two thermocouples placed at both end of the bridge's heatsink. Temperature accuracy is estimated to be within the ±1°C range. More accuracy is not required because of the simplicity of the body diode forward voltage drop model we chose above.

B. Parameter identification

Fig 6 represents the measured drain-to-source voltage when the MOSFET is in the on-state, for 6 different ambient temperatures. As can be seen on fig. 7, the R_{DSon} behaves as a 2nd order polynomial:

$$R_{DSon} = C_0 + C_1 T + C_2 T^2 \tag{13}$$

When fitting data, such a polynomial yields to: $C_2=16\times10^{-8}\ \Omega.T^{-2}$, $C_1=32\times10^{-6}\ \Omega.T^{-1}$, $C_0=58\times10^{-4}\Omega$

The body diode forward-voltage measurement set, shown on fig. 8 is more complex to identify. Linear fit is chosen instead of more powerful math functions as it is more compact to implement in hardware, while giving satisfying results in our case. Fitting is set to minimise error at high current, near SOA (Safe Operation Area) limits, where accuracy is at a premium to keep the converter reliable. As a consequence, error is not negligible at low current. Higher order modelling would be required to reduce this inaccuracy, but is beyond of the scope of the targeted application.

In our case, a very simple expression gives the value of the body diode voltage drop:

$$V_F = V_S(T) + K_2 I$$

The relation between Vs and temperature can be seen on fig. 9 , and is expressed by (6). Body diode forward voltage can therefore be expressed as follow:

$$V_F = K_0 + K_1 T + K_2 I$$

From the identification of data with (7) it comes: $K_2 = 1.9\times10^{-3}\ \Omega$, $K_1 = -1.5\times10^{-3}\ V.K^{-1}$, $K_0 = 0.786$ V

This set of parameters (C_0, C_1, C_2, K_0, K_1, K_2), allows the calculation of temperature and current across the MOSFET by only proceeding to two distinct drain-to-source voltage measurements.

5. Application and discussion

A. Implementation of the method

The method described above is implemented in a microcontroller, to realise a monitoring system that computes temperature and current across one of the MOSFET in an inverter. Two subsystems are required to perform the estimation. A driver board, built around a FPGA (Field Programmable Gate

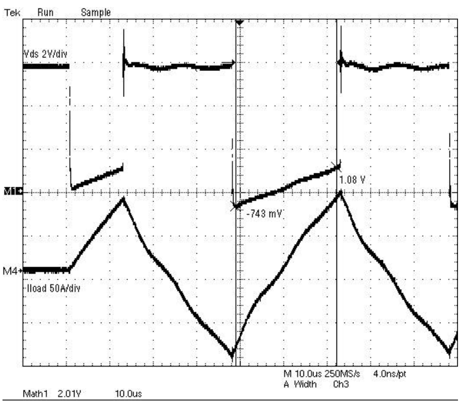

fig. 4 Clamped drain-to-source voltage and corresponding drain current measured by a dedicated probe, showing voltage measurements used for the current and the temperature estimation

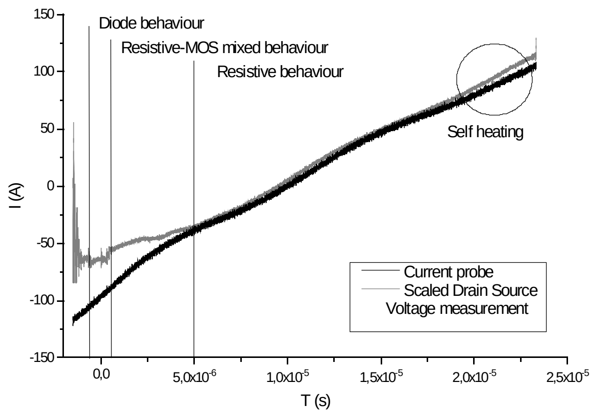

fig. 5 Drain-to-source voltage during the conduction period.

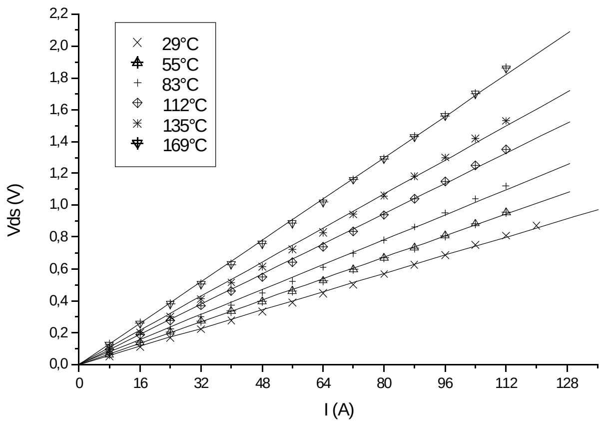

fig. 6. On-state voltage drop for several ambient temperatures

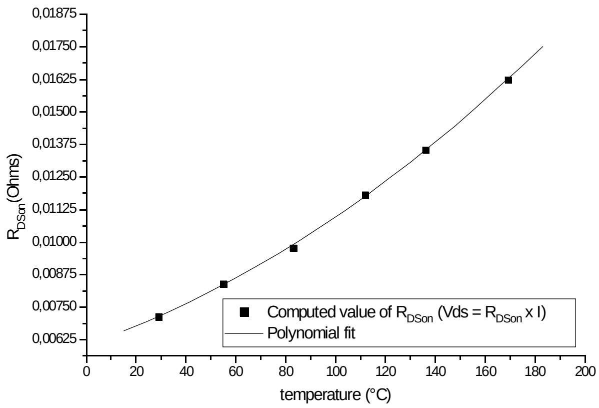

fig. 7. Evolution of the MOSFET on-state resistance as a function of temperature

Array), generates specific driving signals (featuring MOSFET forced freewheeling). Drain-to-source voltage value is acquired by the estimator board, based on a small outline microcontroller, which then outputs temperature and current values.

The acquisition path is made of a differential amplifier, followed by a fast sample and hold amplifier (700 ns blocking delay). This allows the relatively low microcontroller's analog-to-digital converter to be used, avoiding the need for a dedicated high speed converter. Both voltage measurements (V_{DSon} and V_F) are made through the same acquisition path.

The equations described above are implemented into the microcontroller. Built for the sake of demonstration purposes, the experimental setup allows some simplifications. Bridge duty cycle is set to 50%, with a low value inductive load. This results in a pure AC, symmetric triangular-shaped load current. We therefore chose a lapse of time between beginning of the conduction of the monitored MOSFET and V_F voltage acquisition equal to the lapse of time between acquisition of V_{DSon} and the end of conduction. Due to symmetry of the current shape, the current intensity when acquiring V_F and when acquiring V_{DSon} are equals with opposite signs. As $I_1 = -I_2$ (12) becomes:

$$V_{DS1} = -\left(C_0 + C_1 T + C_2 T^2\right) \frac{V_{DS2} + K_0 + K_1 T}{K_2} \tag{14}$$

To figure out the temperature value, the microcontroller solves (14) by using a dichotomy algorithm. Temperature being known, Current comes directly from (11).

B. Results

As the current waveform presents a constant shape, the system can directly display the RMS current value. This allows for precise measurement using the oscilloscope, as it integrates current value over several periods. Peak and RMS current

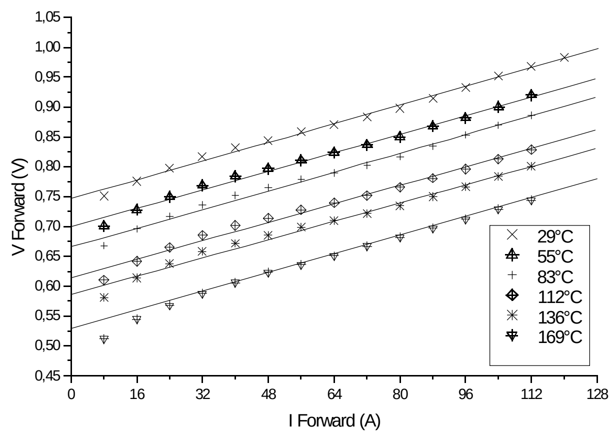

fig. 8. body diode voltage drop for several ambient temperatures

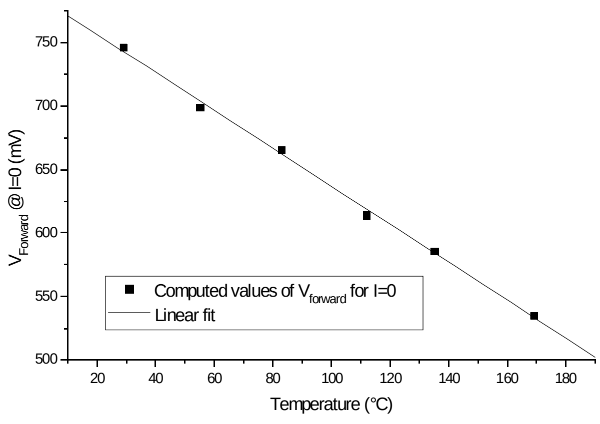

fig. 9. Evolution of the MOSFET body diode threshold voltage as a function of temperature

values are simply proportional in a $\sqrt{3}$ ratio (triangular signal).

Temperature computation requires about 1ms, due to the intense use of floating point 32-bits numbers and the dichotomy algorithm, which requires 8 computations of (12) in the worst case (temperature is coded as an 8-bits integer). Current computation is a lot faster (few tens of µs) as it only requires a single floating point multiply and two additions.

Accuracy of the monitoring system is tested over full current and temperature rating of the MOSFETs. Measurement points are different from those of the parameters estimation (above) to ensure our method is reliable. Driving of the bridge is still made using burst square signals to avoid self-heating that would result in different chip and heatsink temperatures.

The current and temperature estimated by the monitoring system are compared to the values measured by the current probe and the thermometer. Two error maps (see fig. 10 and fig. 11) are given.

On the current estimation error card (fig. 10), one can notice that error is high for low currents. This is mainly due to insufficient resolution of the estimator, which calculates current value as an integer. Error does however never exceed 2 Amps over the whole map.

Temperature estimator error map (fig. 11) is more complex, The hypothesis of proportionality between body diode forward voltage drop and drain current is accurate at high current level (see fig. 8), but as it decreases, the error increases. Fitting of measurement curves is chosen to optimise estimation at high-current (to achieve high reliability), at the cost of reduced accuracy when switching low current.

In addition, it appears that temperature estimation is very sensitive to the forward voltage drop of the body diode. A high resolution measurement of this voltage (such as 14-bit A/D conversion) would be required to increase estimation accuracy.

To prove the system meets its requirements (accurate near SOA limits), a global factor of merit is proposed:

$$\Delta_{I,T} = \sqrt{\Delta_I^2 + \Delta_T^2} \tag{15}$$

where

$$\Delta_x = \frac{x_{measured} - x_{estimated}}{x_{measured}} \tag{16}$$

It is plotted on fig. 12. It can be seen that on the upper right half of the map, values calculated by the estimator have maximal accuracy.

C. Application to thermal impedance measurement

A laboratory application of the estimator is the measurement of thermal impedance. Assuming losses in each transistor are known, as well as internal and ambient temperature, one can calculate the equivalent thermal resistance of the heatsink-substrate-MOSFET assembly shown fig. 13.

$$R_{TH} = \frac{T_{chip} - T_{Ambient}}{P_{losses}} \tag{17}$$

Losses measurement are performed on one of the inverter legs of the bridge, using a calorimetric method [10]. One of the previously used leg is dipped into oil, which temperature rise is measured, while the other is kept out of the calorimeter. The oil tank is placed into a thermally-controlled bath to ensure energy exchange is constant. The overall thermal capacitance of the oil tank (including the bridge leg) is calibrated by dissipating a known power (using a resistor) and by measuring the temperature rise. The inverse process is performed when measuring losses of the bridge leg:

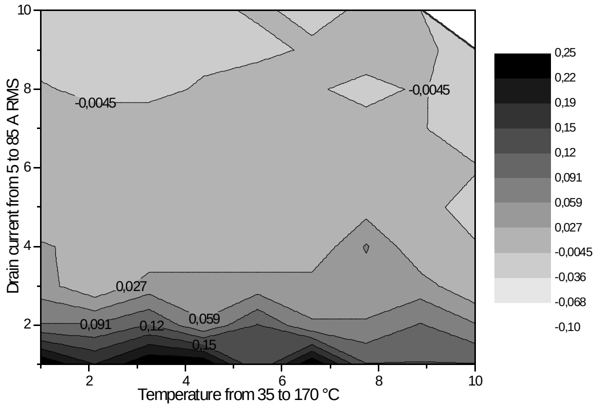

fig. 10 Current estimation error map

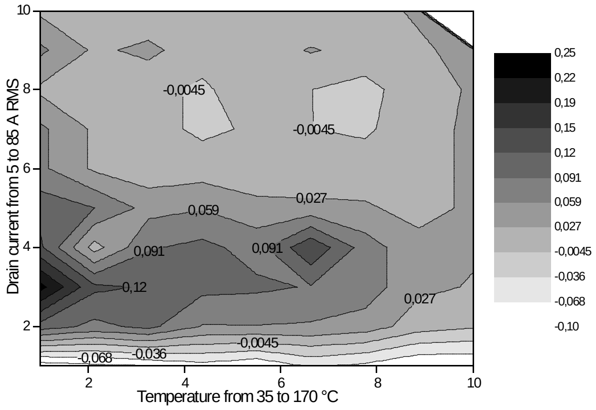

fig. 11 Temperature estimation error map

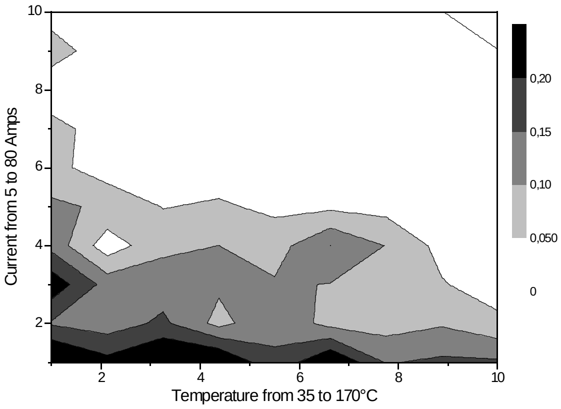

fig. 12 Error map

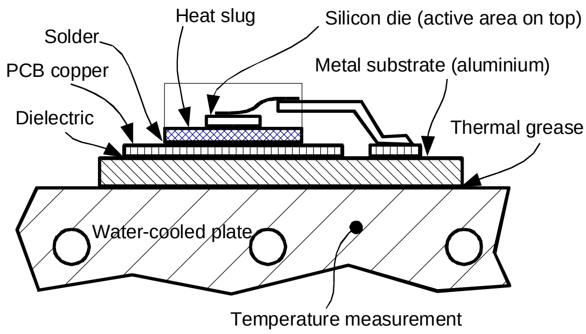

fig. 13 Thermal impedance measurement setup: a D2PAK transistor, mounted on IMS. This assembly is attached to a water-cooled plate

temperature rise is monitored, thermal capacity is now known, dissipated energy can therefore be figured out. As the bridge operates for a precise amount of time, the measured energy yields to losses value (power).

Here, we assume that the only losses of the leg come from the MOSFETs, and each transistor dissipates half the total power. Symmetries in the leg layout as well as in the transistor drives (using DC/DC converters and optic fiber to achieve good isolation) allow for the latter assumption. Losses in connections are not taken into account, although the high load current (up to 150 Amps) makes them not negligible. This will have a detrimental effect on result accuracy, and one cannot expect better than 10%.

The H-bridge is then mounted on a water-cooled plate, and the estimator is used to figure out the internal temperature of one of the transistors. Water cooling is required to ensure the ambient temperature remains constant while dissipated power varies. This imposes some changes in the inverter layout (longer busbar and different MOSFET to estimator-board connection), and again has a detrimental effect on the accuracy.

Table 1 Calculation of thermal impedance from internal temperature, ambient temperature and losses in the transistor.

Supply Voltage	***17.6V***	***19.2V***	***22V***
Total leg losses	45.8W	58.8W	68.8W
Losses per transistor	22.9W	29.4W	34.4W
Estimated Temperature	33°C	39°C	47°C
Ambient temperature	17.8°C	17.8°C	18.2°C
Thermal impedance	0.66°C/W	0.72°C/W	0.84°C/W

As expected, results are strongly affected by the assumptions we made above. Transistors are

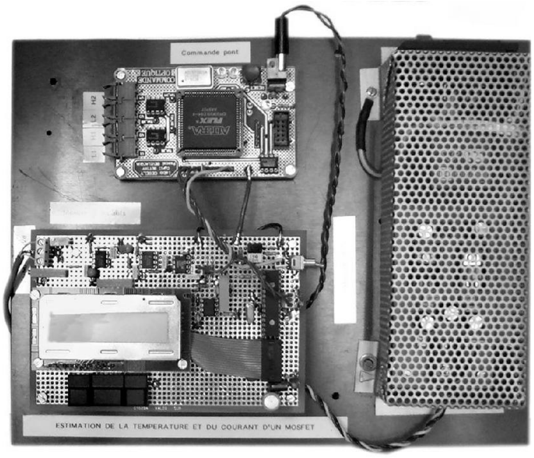

fig. 14 The monitoring system, including bridge drive (top), estimator (bottom) and power supply (right).

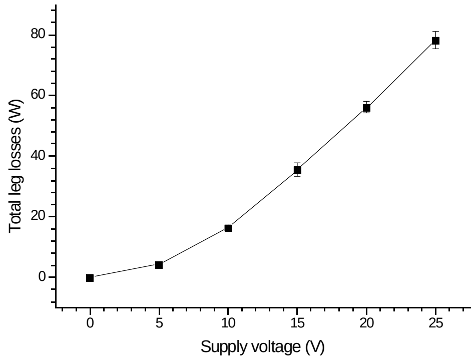

fig. 15. Evolution of leg losses with bridge supply voltage

obviously not the only source of losses (all connections become very hot, proving in a practical way that their losses are not negligible), resulting in 25% dispersion.

6. Further developments and conclusion

The principle of voltage-measurement based estimator for current and temperature in MOSFET H-Bridge is presented in this paper. It exhibits several advantages over usual monitoring systems: It provides the temperature of the active area of the chip , it is integrable in the driver circuitry, and avoids the common pitfalls of high-current sensing.

The proposed method is implemented into a small outline microcontroller board with a single analog acquisition path.

Accuracy of the estimation over full temperature and current range is measured and analysed (error mapping). Confidence maps confirm the reliability of the estimator.

An application to thermal impedance measurement is briefly described, using the estimator along with a calorimetric method. Dispersion of the results is relatively high due to two major experimental difficulties: electrical response change because geometry of the circuit is altered to suit the calorimeter, and calorimetric method gives global losses without the possibility to remove the contribution of power conductors and connectors.

Aimed at industrial converter monitoring, the estimator is however applied to a laboratory experiment. Driving signals (fixed duty cycle) and load (almost pure inductance, with a low value with respect to the switching frequency) are adapted to suit a demonstration purpose only. A few adaptations, mainly software, would allow the proposed method to meet “Real World Applications” particularities.

Thanks to current and temperature properties (long time constant vs. switching frequency, periodic behaviour, isothermal areas...) some assumptions can be made, allowing the implementation of the presented technique in operational converter.

As a conclusion, it is confirmed that the proposed method, based on voltage measurements, allows for the estimation of two key variables in MOSFET-based converters : current and internal chip temperature.

References

[1]. D. Bergogne, B. Allard, H. Morel, “An estimation method of the channel temperature of power MOS devices”, Proceedings of the PESC'00 conference, Galway, 2000, pp 1594-1599.

[2]. B. Allard, H. Morel, K. Ammous, et al., “Application of averaged Models to Real-Time Monitoring of Power Converters”, Proceedings of the PESC'01 conference, Vancouver, pp 486 -491, vol.2.

[3]. A. Ammous, B. Allard, H. Morel, “Transient Temperature Measurements and Modelling of IGBT's under Short Circuit”, IEEE Trans. on Power Electronics, Vol. 13, NO. 1, pp 12-25, 1998

[4]. G. Massobrio, P. Antognetti, “Semiconductor device modelling with SPICE”, New York: McGraw-Hill, Second edition, 475 p.

[5]. F. Profumo, A. Tenconi, S. Facelli, B. Passerini, “instantaneous Junction Temperature Evaluation of High Power Diodes (Thyristors) During Current Transients”, IEEE Trans. On Power Electronics, Vol. 14, NO. 2, March 1999, p 292-299

[6]. A.Maxim, G. Maxim, D. Andreu, J. Boucher, “Power PIN Diode Electro-Thermal SPICE Macromodel with Forward and Reverse Recovery”, Proceedings of the EPE'99 conference, Lausanne, 1999.

[7]. A. Muñoz-Yagüe, P. Leturcq, “High Level Behavior of Power Rectifiers: A Quantitative Analysis of the Forward Voltage Drop”, IEEE Trans. On Electron Devices, Vol. ED25, NO 1, January 1978

[8]. B. J. Baliga, “Modern Power Devices”, John Wiley & Sons, 1987

[9]. Dr. Martin März, Paul Nance “Thermal Modeling of Power-electronic Systems”, Infineon Technologies AG, Munich, available online: http://www.infineon.com/cmc_upload/migrated_files/document_files/Application_Notes/mmpn_eng.pdf

[10]. Bruno ALLARD, Hervé MOREL, Kaiçar AMMOUS, et al. “Design of a calorimetric system using bond graphs.”, Proceedings of the ICBGB 2001 Conference, Phoenix, Arizona, January 2001.